

An Original Supramolecular Helicate from a Bipyridine–Bipyrazine Ligand Strand and Ni^{II} by Self-Assembly

Julien Mathieu,^[a] Bernard Fraisse,^[b] Daniel Lacour,^[d] Nouredine Ghermani,^[c] François Montaigne,^[d] and Alain Marsura*^[a]

Dedicated to the memory of Professor Claude Selve

Keywords: Magnetic properties / N ligands / Nickel / Self assembly / Supramolecular chemistry

A new discrete supramolecular pseudo-helicate has been obtained from a saturated heterotopic methylbipyrazyl–methylbipyridyl ligand strand and NiCl₂. The X-ray structure of the dinuclear complex shows the 2-oxapropylene bridge oxygen atoms are engaged in coordination to the octahedral metal centre and a selective ligand inter-strand orientation is promoted in the complex. The crystal packing shows a perfect regular linear arrangement of the asymmetric units giving a

packing of interacting molecules having well-defined rectangular and polygonal open channels. Although a paramagnetic behaviour is observed above 10 K, below this temperature a significant deviation of this behaviour suggests the presence of an Ni^{II}–Ni^{II} magnetic coupling.

(© Wiley-VCH Verlag GmbH & Co. KGaA, 69451 Weinheim, Germany, 2006)

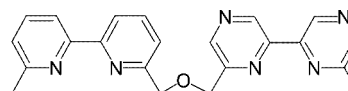
Introduction

Over the last ten years of intensive research, numerous supramolecular architectures obtained by self-assembly processes have been reported in the literature, and several reviews^[1–6] give an overview of these compounds and their properties. Looking at exploratory investigations, one can see that the didentate heterocyclic 2,2'-bipyridine ligand has played a central role in the spontaneous formation of the main, from simple to sophisticated, supramolecular inorganic architectures.^[7,8] A variety of discrete and highly organised species have been obtained by means of ligands designed to afford a well-defined architecture of a single type

with given metal ions.^[7,8] Famous examples in the literature involve oligobipyridine strands, which lead to double-stranded, triple-stranded or circular helical complexes depending on the metal ion coordination geometry and the nature of the spacer between the bipyridine nuclei.^[9–12] Recently, we have studied the self-assembly of sequential 2-oxapropylene-bridged bipyridine–bidiazine ligand strands with tetracoordinate metal ions into selectively oriented H–H (head-to-head) or H–T (head-to-tail) double-stranded helicates.^[13,14]

Results and Discussion

As far as we know no supramolecular inorganic architectures obtained by spontaneous self-assembly of sequential 2-oxapropylene-bridged bipyridine–bidiazine ligand strands with an Ni^{II} cation have been reported in the literature. The formation of the metal complexes was monitored by UV/Vis spectrophotometric titration of a solution of the heterotopic bipyridine–bipyrazine ligand **1**^[13,14] at room temp. with NiCl₂ (Figure 1) in dry acetonitrile.



Ligand 1

- [a] GEVSM, UMR CNRS 7565; Structure et Réactivité des Systèmes Moléculaires Complexes, Université Henri Poincaré Nancy-1, 5, rue A. Lebrun, B. P. 403, 54250 Nancy Cedex, France
Fax: +33-3-8368-2345
E-mail: Alain.Marsura@pharma.uhp-nancy.fr
- [b] Laboratoire SPMS UMR CNRS 8580, Ecole Centrale Paris, 1, Grande Voie des Vignes, 92295 Châtenay-Malabry, France
Fax: +33-1-4113-1437
E-mail: fraisse@spms.ecp.fr
- [c] Laboratoire de Physique Pharmaceutique UMR 8612 Université Paris XI, Faculté de Pharmacie 5, Rue J. B. Clément, 92296 Châtenay-Malabry Cedex, France
Fax: +33-1-46835882
E-mail: noureddine.ghermani@cep.u-psud.fr
- [d] Laboratoire de Physique des Matériaux, UMR 7556, Université Henri Poincaré Nancy-1, Faculté des Sciences, Bd des Aiguillettes B. P. 239, 54506 Vandoeuvre-les-Nancy Cedex, France
Fax: +33-3-83684801
E-mail: montaigne@lpm.u-nancy.fr

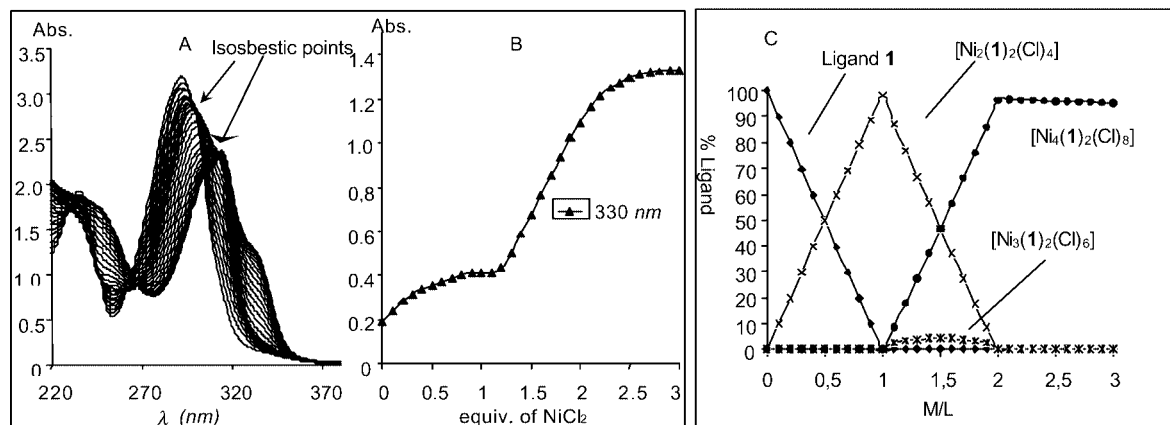


Figure 1. Spectrophotometric titration of the ligand **1** (10^{-4} M) with NiCl_2 (6×10^{-3} M) in MeCN: (A) UV/Vis absorption spectra; (B) plot of absorbance vs. added salt at 330 nm; (C) calculated ligand speciation curves in CH_3CN for ligand **1** and $[\text{Ni}^{\text{II}}/\text{ligand } \mathbf{1}]$ in the range 0.1–3.0.

The titration spectra of ligand **1** display two successive isosbestic points between 220 and 400 nm over the complete titration range. On the addition of NiCl_2 , a red shift of the absorption spectrum occurs, and a strong absorption and a marked shoulder appear distinctly and successively at $\lambda_{\text{max}} = 315$ ($\epsilon = 21500$) and 333 nm ($\epsilon = 12600$), thereby indicating the effective coordination of the Ni^{II} ions. The titration plot [Figure 1(B)] shows the formation of a first species with a composition of approximately one Ni ion for 1 equiv. of **1**, in agreement with the X-ray structure of the isolated nickel complex **2**. This is followed by the appearance of a second species upon addition of a second equivalent of Ni^{II} to reach a composition of about two Ni atoms for every equivalent of **1**. UV titration and analysis of the data indicate that the second species could be the complex $[\text{Ni}_4(\mathbf{1})_2\text{Cl}_8]$, which corresponds to coordination of the remaining nitrogen sites (Figure 2). The binding constants $\log(\beta_m)$ for the species M_mL_l were calculated with the SPECFIT program:^[15] $[\text{Ni}_2(\mathbf{1})_2\text{Cl}_4]$ $\log(\beta_{22}) = 34.5 \pm 0.5$; $[\text{Ni}_3(\mathbf{1})_2\text{Cl}_6]$ $\log(\beta_{32}) = 41.6 \pm 1.4$; $[\text{Ni}_4(\mathbf{1})_2\text{Cl}_8]$ $\log(\beta_{42}) = 51.0 \pm 2.3$. The distribution curves computed from the formation constants show that the $[\text{Ni}_2(\mathbf{1})_2\text{Cl}_4]$ and $[\text{Ni}_4(\mathbf{1})_2\text{Cl}_8]$ complexes are formed quantitatively for $\text{M/L} = 1$ and 2, respectively. According to the speciation [Figure 1(C)], the formation of $[\text{Ni}_3(\mathbf{1})_2\text{Cl}_6]$ can be neglected.



Figure 2. Proposed structure of the complex $[\text{Ni}_4(\mathbf{1})_2\text{Cl}_8]$.

ES-MS studies of the MeCN or CH_2Cl_2 solutions revealed the presence of ions that could be assigned to

$[\{\text{Ni}_2(\mathbf{1})_2\text{Cl}_2\}]^{2+}$, $[\{\text{Ni}_2(\mathbf{1})_2\text{Cl}_3\}]^+$ and $[\{\text{Ni}_3(\mathbf{1})_2\text{Cl}_5\}]^+$ (all charges were confirmed by partial mass isotopomer distributions and corresponding simulated profiles). This shows unambiguously that the discrete complex **2** contains two ligands and two Ni^{II} ions.

The Ni complex **2** crystallises in the centrosymmetric $P\bar{1}$ space group. The asymmetric unit contains one nickel ion, one bipyridine (bpy) and one bipyrazine (bpz) ligand. The two parts of the dinuclear Ni helicate are related by a centre of inversion, as shown in the ORTEP^[16] diagram (Figure 3). In this double-stranded complex, each Ni ion is in a pseudo-octahedral coordination that involves two chlorine anions, two nitrogen atoms of the bipyridine ligand, one nitrogen atom of the bipyrazine molecule and the bridging oxygen atom, which means that the bpz N4, N5 and N6 nitrogen atoms are not connected to any metal centre. The metal–ligand bonds are Ni–N1 = 2.010(6), Ni–N2 = 2.113(5), Ni–N3 = 2.242(7), Ni–O1 = 2.290(5), Ni–Cl2 = 2.327(2) and Ni–Cl1 = 2.369(2) Å.

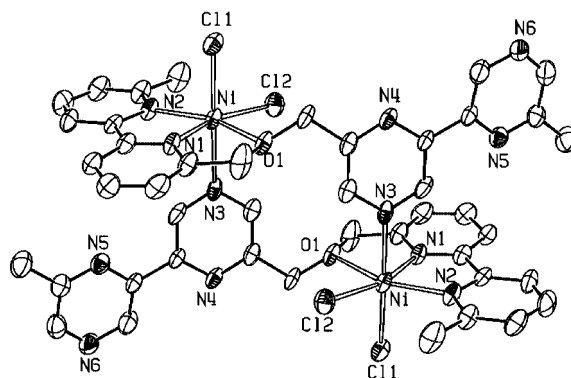


Figure 3. ORTEP drawing of the Ni^{II} complex (H atoms have been omitted for clarity). Thermal ellipsoids are at the 50% probability level.

The distorted octahedra of Ni are characterised by internal angles varying from $74.9(2)^\circ$ (N1–Ni–O1) to $94.7(1)^\circ$ (Cl1–Ni–Cl2). In comparison, Ni–N bonds with bpy ligands are found in the range from 2.060 to 2.078 Å in the

bis[3,6-(dipyrid-2-ylmethyl)pyridazine]nickel dinuclear helicate,^[17] where the metal ion is also octahedrally coordinated. In our Ni complex, the bpy ligand is rigorously planar whereas the bpz one has an N5–C–N4 torsion angle of $-162.4(7)^\circ$ (see Figure 3). The metal–metal distance in our Ni complex is 6.96 Å and is much longer than those found in our previous Ag and Cu helicate structures.^[13,14] Figure 4 depicts the crystal packing of the (bpy–bpz)Ni complex. The regular linear arrangement of the helicates

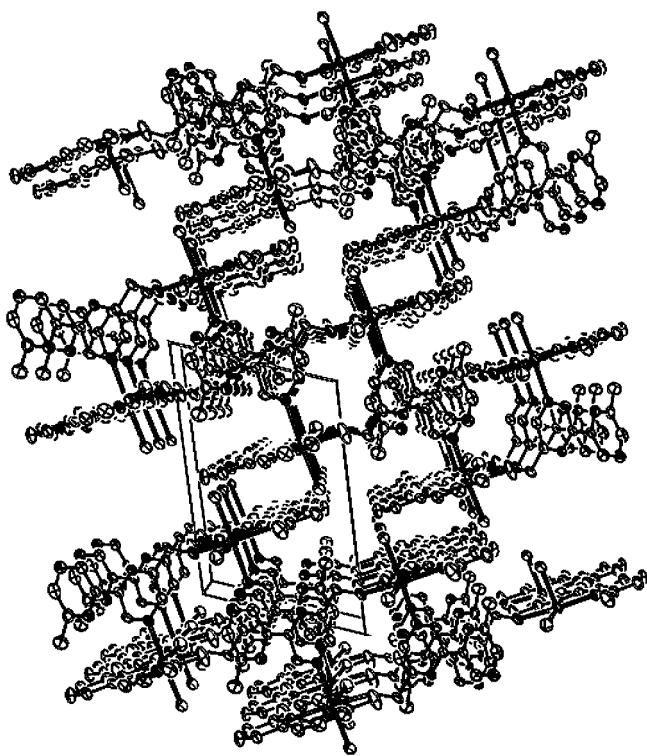


Figure 4. Crystal packing viewed along the *b* axis (Ni bonds are in bold).

along the *b* axis gives rise to open rectangular and polygonal channels in the structure. The closest ligand distances found are between two bpy moieties (5.96 Å).

Monocrystal Magnetic Properties

Both the magnetic moment and the AC and DC magnetic susceptibility (χ) of single crystals of the nickel complex **2** were investigated from 2 K to room temperature. Above 100 K the sample magnetic moment is lower than the diamagnetic signal originating from the sample holder and so is close to zero ($< 2 \times 10^{-7} \text{ Am}^2$). A plot of the χT product vs. *T* is shown in Figure 5(A) for temperatures between 2 K and 100 K. Figure 5(B) presents the measured magnetic moment vs. the field/temperature ratio for different applied fields and temperatures. The χT product is constant from 100 K to about 10 K and the magnetic moment vs. the field/temperature ratio curves are superimposed. This suggests a simple paramagnetic behaviour in this temperature range. Below 10 K, χT varies strongly with the temperature, indicating that the sample is not in a paramagnetic regime anymore. This is confirmed by the data set presented in Figure 5(B). Indeed, the magnetic moment vs. the field/temperature curves are not superimposed anymore below 10 K. The continuous line presented in Figure 5(B) is the Brillouin function calculated for two isolated $S = 1$ nuclei with a Landé factor of $g = 2.57$. Below 10 K, the measured magnetic moment is always smaller than expected, suggesting an antiferromagnetic interaction.

Recently, weak magnetic exchange between two Ni^{II} metal centres operating in some diazine complexes over six bonds and over large Ni–Ni internuclear distances up to 6.6 Å has been reported.^[18] It is interesting to note that such a weak coupling is maintained at higher internuclear distances in our case, with values of 6.9 Å for the intra-helicate Ni–Ni distance and up to 9.4 Å for the inter-helicate distance.

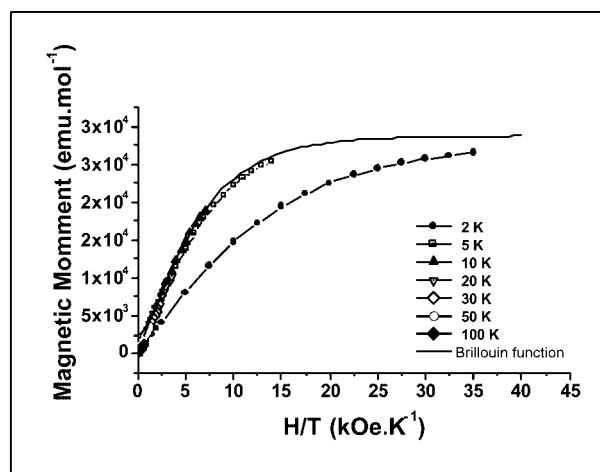
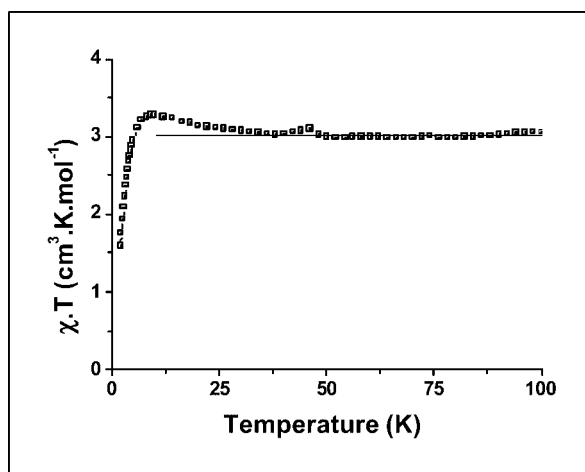


Figure 5. (A, left) DC magnetic susceptibility temperature product vs. temperature. The straight line corresponds to the behaviour expected in a paramagnetic regime. (B, right) Magnetic moment vs. applied field/temperature ratio for different temperatures. The lines between dots are guides for the eyes. The continuous line corresponds to a Brillouin function calculated for two isolated $S = 1$ nuclei (see text).

Conclusions

In contrast to previously reported double-stranded helicates, afforded by the self-assembly of tetracoordinate cations and homotopic or heterotopic bis(didentate) ligands, the nickel cation gives a new discrete assembly involving oxygen atoms of the 2-oxapropylene bridges and two chlorine atoms in a hexacoordinate mode with the metal ion, and so satisfies the “maximum occupation of sites” principle. Moreover, as observed previously with the same heterotopic sequence,^[13,14] one can notice a selective inter-strand orientation which promotes exclusively Ni^{II} coordination between a bipyrazine and a bipyridine unit in the system. From a magnetic point of view, both observation of a simple paramagnetic behaviour and the deviation from this behaviour below 10 K suggest the presence of a weak, antiferromagnetic Ni^{II}–Ni^{II} interaction. In light of these first results, and in order to build a new library of supramolecular systems, complexation studies with other ligands and potentially hexacoordinated metal centres along with deeper investigations of their physical properties are now underway.

Experimental Section

General Remarks: The synthesis of heterotopic ligand **1** has been described by us previously.^[13] UV/Vis spectra were recorded with a UVmC² Safas spectrometer. Mass spectra (ES) were recorded with a Micromass Platform spectrometer. Elemental analyses were obtained with a Perkin–Elmer 240C CHN–O–S analyser.

[Ni₂(1)₂Cl₄] (2): NiCl₂·6H₂O (31 mg, 0.13 mmol) was added to the ligand **1** (50 mg, 0.13 mmol) in anhydrous CH₃CN (10 mL) under argon. The green solution was stirred at room temp. and, after evaporation of the solvent, the solid residue was crystallised by slow diffusion of diethyl ether into an acetonitrile/chloroform solution. After 2 d, suitable green crystals were obtained. UV/Vis (CH₃CN): λ_{max} (ϵ) = 298 nm (28300), 315 (23500), 333 (shoulder) (12600). ESI MS: m/z = 1122.2 [{Ni₃(1)₂Cl₅}]⁺, 992.6 [{Ni₂(1)₂Cl₃}]⁺, 478.6 [{Ni₂(1)₂Cl₂}]²⁺. C₄₄H₄₀Cl₄N₁₂Ni₂O₂ (1029.4): calcd. C 51.29, H 3.88, N 16.32; found C 50.85, H 3.95, N 15.97.

Magnetic Measurements: Both the magnetic moment and the DC magnetic susceptibility (χ) of single crystals of the Ni²⁺ pseudo-helicate were investigated from 2 K up to room temperature. The sample mass was 2.4 mg. The magnetic moment evolution with temperature (denoted T as mentioned above) was monitored by SQUID magnetometry in a magnetic field of 0.1 T. The small magnetic contribution originating from the substrate holder was subtracted from the analysed data.

X-ray Crystallographic Study: The crystal structure of C₄₄H₄₀Cl₄N₁₂Ni₂O₂ [$\rho_{\text{calcd.}}$ = 1.61 g cm^{−3}, $\mu(\text{Mo–K}\alpha)$ = 1.19 mm^{−1}] was determined from a single-crystal X-ray diffraction experiment performed with an Enraf–Nonius CAD-4F diffractometer (Mo–K α radiation, λ = 0.71073 Å) at room temperature. A large crystal (green, 0.60 × 0.50 × 0.30 mm) was chosen for the experiments. The compound crystallised in the triclinic space group $P\bar{1}$, Z = 1. The unit-cell parameters were obtained by least-squares fit to setting angles of 25 reflections in the range 8° < 2θ < 30°. Cell parameters: a = 8.647(2), b = 10.063(8), c = 13.658(4) Å, α = 106.78(4)°, β = 106.76(2)°, γ = 96.98(4)°, V = 1062(1) Å³. The ω – 2θ scan mode was used to record the diffraction intensities. Three standard reflections

were monitored every 2 h in order to control the intensity decay, which did not occur significantly. 6409 reflections were collected up to $2\theta_{\text{max}}$ = 59.96°. Lorentz-polarisation corrections and data reduction were performed using the WINGX package^[19] for CAD4 collected intensities. The structures were solved by direct methods using the SIR92 program^[20] and refined by the full-matrix least squares based on F^2 using SHELX97.^[21] Thermal displacements of non-hydrogen atoms were refined anisotropically. Hydrogen atoms were included at their idealised positions. During the last cycles of refinement, the best results were obtained with empirical absorption corrections using the XABS2 program in the WINGX package.^[19] The final statistical factors were $R1(\text{all data})$ = 0.214, $wR2$ = 0.308 for 6166 data and 289 parameters, $R1[F^2 > 2\sigma(I)]$ = 0.0906 for 3009 data with $F^2 > 2\sigma(I)$ and the final residual densities in the unit cell were +1.47 and −1.66 e Å^{−3}. CCDC-234807 contains the supplementary crystallographic data for this paper. These data can be obtained free of charge from The Cambridge Crystallographic Data Centre via www.ccdc.cam.ac.uk/data_request/cif.

Acknowledgments

We would like to thank the French MESR and the CNRS for support, J. M. Ziegler and D. Bouchu for recording the mass spectra, and Mrs. N. Marshall for correcting the manuscript.

- [1] J.-M. Lehn, *Supramolecular Chemistry*, VCH, Weinheim, **1995**.
- [2] A. F. Williams, *Chem. Eur. J.* **1997**, *3*, 15–25.
- [3] M. Albrecht, *Chem. Rev.* **2001**, *101*, 3457–3497.
- [4] M. D. Ward, *Annu. Rep. Prog. Chem. Sec. A* **2000**, *96*, 345–385.
- [5] J.-M. Lehn, *Chem. Eur. J.* **2000**, *6*, 2097–2102.
- [6] C. Piguet, G. Bernardinelli, G. Hopfgartner, *Chem. Rev.* **1997**, *97*, 2005–2062.
- [7] C. Kaes, A. Katz, M. W. Hosseini, *Chem. Rev.* **2000**, *100*, 3553–3590 and references cited therein.
- [8] D. P. Funeriu, J.-M. Lehn, K. M. Fromm, D. Fenske, *Chem. Eur. J.* **2000**, *6*, 2103–2111.
- [9] R. Kramer, J.-M. Lehn, A. Marquis-Rigault, *Proc. Natl. Acad. Sci. USA* **1993**, *90*, 5394–5398.
- [10] B. Hasenknopf, J.-M. Lehn, N. Boumediene, E. Leize, A. van Dorsselaer, *Angew. Chem. Int. Ed.* **1998**, *37*, 3265–3268.
- [11] B. Hasenknopf, J.-M. Lehn, N. Boumediene, A. Dupont-Gervais, A. van Dorsselaer, B. Kneisel, D. Fenske, *J. Am. Chem. Soc.* **1997**, *119*, 10956–10962.
- [12] B. Hasenknopf, J.-M. Lehn, B. Kneisel, G. Baum, D. Fenske, *Angew. Chem. Int. Ed. Engl.* **1996**, *35*, 1838.
- [13] J. Mathieu, A. Marsura, N. Bouhaida, N. Ghermani, *Eur. J. Inorg. Chem.* **2002**, 2433–2437.
- [14] J. Mathieu, N. Ghermani, N. Bouhaida, B. Fenet, A. Marsura, *Eur. J. Inorg. Chem.* **2004**, 5338–5346.
- [15] Log β values were calculated using the SPECFIT[®] program v3.0, Spectrum Software Associates, **1993–2001**.
- [16] M. N. Burnett, C. K. Johnson, ORTEP-III report ORNL-6895, **1996**, Oak Ridge International Laboratory, Tennessee, USA.
- [17] C. J. Sumby, P. J. Steel, *Inorg. Chem. Commun.* **2003**, *6*, 127–130.
- [18] Z. Xu, L. K. Thompson, V. A. Milway, L. Zhao, T. Kelly, D. O. Miller, *Inorg. Chem.* **2003**, *42*, 2950–2959.
- [19] L. J. Farrugia, *J. Appl. Crystallogr.* **1999**, *32*, 837–838.
- [20] A. Altomare, G. Casciaro, C. Giacovazzo, A. Guagliardi, *J. Appl. Crystallogr.* **1993**, *26*, 343–350.
- [21] G. M. Sheldrick, *SHELXL97 and SHELXS97, Program for the Refinement of Crystal Structures*, University of Göttingen, Germany, **1997**.

Received: July 25, 2005

Published Online: November 22, 2005